



# Upscaling colloidal transport from the column to the field: The value of a large gravel column experiment as an intermediate step

M. E. Stevenson<sup>1,2</sup> · T. J. Oudega<sup>1,2</sup> · G. Lindner<sup>2,3</sup> · R. Sommer<sup>2,3</sup> · A. K. T. Kirschner<sup>2,3</sup> · A. Scheidl<sup>4</sup> · A. Eder<sup>4</sup> · P. Strauss<sup>4</sup> · G. Blöschl<sup>1</sup> · A. P. Blaschke<sup>1,2</sup>

Received: 6 August 2024 / Accepted: 13 April 2025 / Published online: 5 May 2025  
© The Author(s) 2025

## Abstract

Due to public health or environmental concerns, examining the effects of preferential flow processes on the transport of pathogenic microorganisms or contaminants of emerging concern must be studied in the laboratory. However, the resulting transport parameters cannot be directly applied to field-scale groundwater models. This research explores how an upscaling relationship, with removal as a function of distance, can be found using *B. subtilis* spores and microspheres as colloidal tracers in saturated flow-through experiments at three different scales. The study investigates transport processes in a 4-m-tall undisturbed gravel column and compares the results with previously published data. Results showed that colloidal removal (log-removal, attachment rate/efficiency) in heterogeneous porous media follows a power law as a function of travel distance, rather than an exponential relationship, which is normally assumed in removal equations. It was found that by using a power function, it was possible to decrease the difference between the attachment coefficients so that the meso-scale value was closer to the small-scale value. To the contrary, using a dual permeability model increased the difference between attachment rates at these two scales. Groundwater transport modeling may benefit from taking this power law relationship into account, instead of using a constant first-order removal rate, as most tracer tests are performed at a smaller scale than the scale that is being modeled. The meso-scale column provides insights into upscaling processes by incorporating an intermediate step when comparing groundwater transport at the column scale to the field scale.

**Keywords** Heterogeneity · Scale effects · Tracer tests · Colloidal transport · Preferential flow

---

This article originates from the International Association of Hydrogeologists (IAH) 50th Worldwide Groundwater Congress, Cape Town, South Africa, 17–22 September 2023, which was jointly organized by the Ground Water Division of the Geological Society of South Africa and the South African Chapter of the IAH.

---

✉ M. E. Stevenson  
stevenson@hydro.tuwien.ac.at

<sup>1</sup> Institute of Hydraulic Engineering and Water Resources Management, Vienna University of Technology, Karlsplatz 13, 1040 Vienna, Austria

<sup>2</sup> Interuniversity Cooperation Centre Water and Health, Vienna, Austria

<sup>3</sup> Institute for Hygiene and Applied Immunology, Medical University of Vienna, Kinderspitalgasse 15, 1090 Vienna, Austria

<sup>4</sup> Institute for Land and Water Management Research, Federal Agency of Water Management, Pollnbergstrasse 1, 3252 Petzenkirchen, Austria

## Introduction

A conundrum in groundwater modeling, and hydrological modeling in general, is the paradox created by requiring a measurement scale, a modeling scale and the presence of a natural process scale (Blöschl and Sivapalan 1995). A measurement scale is required for practical purposes, for example, in groundwater tracer tests are constrained by the available piezometer distances at a field site or what influent concentration is allowed by permitting authorities. The modeling scale depends on the problem definition from the client or research project, e.g., what is the setback distance for a particular drinking water well at a particular location. Therefore, the spatial extent of a groundwater model depends on the specific objectives of the study, rather than capturing the natural processes, such as preferential flow paths. The process scale is what drives and creates the groundwater flow paths and is defined by nature itself. In a perfect world, these three scales would be on the same order of magnitude;

however, the field measurement scale for groundwater contaminant transport is usually on the order of magnitude of 10–1000 m (Fogg and Zhang 2016), while the modeling scale required is usually 0.1–100 km (transport distance). On the extreme end of the spectrum, even global groundwater models exist (de Graaf et al. 2015). The process scale is variable and site-dependent, but could also be on the order of magnitude of 0.1–100 km. Therefore, there is the problem that the measurement scale does not reflect what is required for modeling, nor what is happening in nature. This begs the question: can groundwater transport processes be observed at the measurement scale and upscaled to the modeling scale?

This lofty goal may be achievable in a perfectly isotropic, homogeneous aquifer with spherical, smooth sand grains. Of course, no such natural aquifer exists, and some degree of preferential flow is inevitably present, demonstrated by conservative tracer tests exhibiting asymmetrical breakthrough curves with tailing, even in fairly homogeneous aquifers (Harvey et al. 1993; Mackay et al. 1994). It may be reasonable to assume that preferential flow in the subsurface is possibly the rule, rather than the exception. Preferential flow, defined as non-equilibrium flow behavior due to bypass flow that is caused by physical cracks or zones of relatively higher conductivity, was first mentioned in a publication by Lawes, Gilbert and Warington in 1882 (Gish and Shirmohammadi 1991). Later, Theis, wrote: “It seems obvious that mixing processes are involved in real aquifers that are not reproduced in dispersion experiments in the laboratory. It also seems obvious that the heterogeneous character of clastic sediments and other porous rocks must be involved in these mixing processes.” (Theis 1967).

Traditional groundwater modeling is done with the finite difference or finite element method (Freeze and Cherry 1979), and is based on the assumption of the ergodic behavior of groundwater in the subsurface and the concept of a representative elementary volume (REV), also called a representative volume element (RVE). This is considered the smallest area or volume for which a measurement can be considered representative (Du and Ostojca-Starzewski 2006). The volume at which the REV is representative depends on the scale being considered, and the threshold at which fluctuations of the property value at the microscopic scale stabilize, and the value becomes constant at the macroscopic (Darcy) scale. For heterogeneous material, this value diverges again with distance (Bear 1972). For practicality of groundwater modeling, this usually means making generalizations about the extent of porosity and measured hydraulic conductivity values, the area of which is assumed to be large enough to take minor heterogeneities into account but, at the same time, small enough to represent major heterogeneities (minor and major being undefined but subject to opinion), or for which the area is homogeneously heterogeneous (Smith

and Freeze 1979). For homogeneous porous material, these assumptions may hold true; however, non-ergodic behavior seems to be prevalent in highly heterogeneous porous material, and this results in stagnant areas and fingering due to non-equilibrium flow or preferential flow (Fiori et al. 2019). The state-of-the-art for modeling heterogeneity is using a stochastic distribution of hydraulic conductivity to make an educated guess about what is happening in the subsurface, based on measurements and geological knowledge of the field site, but this may not be effective due to lack of a proper method for modeling preferential flow at various scales (Fogg and Zhang 2016). To make the situation more complicated, preferential flow may not only follow connected areas of high conductivity but may also travel through areas of low conductivity, in order to connect the high-velocity zones (Bianchi et al. 2011).

The distribution of aquitards and low-permeability materials, which can be easily assessed with laboratory tests such as permeability tests of cores or grain-size distribution curve methods (Hazen, Bayer, etc.), or borehole flowmeter measurements (Fogg and Zhang 2016), are key to understanding the extent of connected flow regions. Interconnectivity is especially important for colloid transport in groundwater. Perhaps the exaggerated preferential flow paths that are observed in colloidal transport, due to size exclusion from small pore spaces, can shed light on solute transport as well, for which preferential flow may be more elusive and not apparent at first glance, with dye tracers being the exception (Ghodrati and Jury 1990).

Removal of colloids during subsurface transport has become an important area of research, being a pre-treatment step in water treatment technologies as well as an important aspect of riverbank filtration. Colloids are defined as any particle in the micron and sub-micron scale that can be transported in a fluid. These could include, for example, clay particles, microorganisms, sediment, or microplastics, all of which are important to study due to potential environmental and human health concerns. Colloidal particles can behave quite differently under varying chemical conditions (Stevenson et al. 2015). Attachment and detachment of colloids in groundwater are extremely complex and poorly understood because it depends on several physiochemical properties of the colloid (size, surface charge, surface macromolecules, density, and morphology) and the porous media (grain size, heterogeneity, chemical composition, and angularity), as well as the groundwater chemistry (i.e., ionic strength and pH). Few studies directly focus on colloidal transport at different scales. Hijnen et al. (2005) conclude that the removal of microorganisms in small-column tests cannot be simply extrapolated to the field, while Knappett et al. (2014) see promise in using laboratory-scale results for predicting field transport if reversible and irreversible attachment of colloids

is incorporated in the modeling. In an extensive review, Pang (2009) hypothesizes that varying rates of colloidal removal may depend on organic matter content, reversible attachment, microbial population heterogeneity, groundwater chemistry (ionic strength) and straining.

Dispersivity of solutes increases with scale (Gelhar et al. 1992), most likely due to fractal geometry in the subsurface (Wheatcraft and Tyler 1988) and heterogeneity causing velocity field fluctuations (Ptak et al. 2004). Moreover, hydraulic conductivity increases with scale in heterogeneous aquifers (Boggs and Adams 1992; Schulze-Makuch et al. 1999), although this theory has been questioned (Hunt 2003). It has been proposed that what is lacking in the field of research on colloidal transport in groundwater are studies at an appropriate scale, representing field conditions and heterogeneities in the underground (Bradford and Harvey 2017). In field-scale studies, there is a decrease in the removal rate of colloids with distance (DeBorde et al. 1998; Dong et al. 2006; Pieper et al. 1997), as well as at the laboratory scale, using small columns (Harter et al. 2000). It is noteworthy that even in small columns of artificially homogeneous glass beads, the removal of colloids decreases with distance, even with influent solutions at various ionic strengths (Tufenkji 2006). Schijven and Hassanizadeh (2000) conclude that virus removal rates decrease with distance and possibilities to upscale need to be investigated. Not only is the present discussion relevant to colloidal transport, the famous MADE experiment (Boggs et al. 1992) in a highly heterogeneous aquifer, using a conservative tracer, found increasingly incomplete tracer breakthrough with distance and asymmetrical breakthrough curves, with heavy tailing. Initially, the measured conservative tracer mass was higher than expected near the injection point, and the tracer recovery decreased with distance (Boggs and Adams 1992), similar to what is observed with colloidal transport. When no single scale is the correct scale and no representative or characteristic transport distance can be found, meaning the transport distance is not finite and extraordinarily long flow times and paths are possible, the flow path may be fractal (Redman et al. 2001; Wheatcraft and Tyler 1988). This is possibly due to the release of solutes from immobile zones having a waiting time (Schumer et al. 2003). A fractal is a pattern that can repeat itself to infinity at various scales, which means that fractals are scale-free and are mathematically described by the power law. The power law implies that a certain variable quantity is proportional to another variable quantity raised to a power,  $\beta$ , such that  $\beta$  cannot be an integer and the data points of such a relationship, plotted on a log–log graph, follow a straight line. Traditional one-site kinetic models of solute transport in groundwater, derived from small-column experiments (Cameron and Klute 1977; Lapidus and Amundson 1952), which follow an exponential law (i.e., a constant is raised to a variable), may be outdated.

It has already been established that colloidal removal processes (attachment rate) are not constant and that a dynamic attachment rate (following a power law) is necessary (Johnson and Elimelech 1995). Traditionally, this is thought to be due to physical and chemical heterogeneity of the porous media and population heterogeneity and motility of microorganisms (Lutterodt et al. 2009; Schijven and Hassanizadeh 2000; Simoni et al. 1998). Although several studies have done colloidal transport experiments in meso-scale (> 1 m) columns (Close et al. 2006; Lutterodt et al. 2009, 2011), the studies did not compare the results to similar porous media at multiple scales. Close et al. (2006) concluded that the removal rate in a meso-scale saturated gravel column (1–8 m) was constant and, therefore, the removal rate could be used to calculate setback distances, which may be misleading, as the experiment was not compared to another scale. The aim of this paper is to explore the possibilities of upscaling colloidal transport and to elucidate the potentially dominant process involved, for example, whether preferential flow is causing the apparent scale-dependent behavior of colloidal removal. There are three ways to do upscaling: deterministic (dimensional techniques), stochastic (statistical techniques), and fractals (Bloeschl and Sivapalan 1995). This paper deals with deterministic scaling (i.e., finding similarities at different scales), in order to show that colloidal removal follows a power law in heterogeneous porous media.

## Methods

### Colloids

*Bacillus subtilis* (ATCC 6633) spores (henceforth referred to as *B. subtilis*), a non-reactive surrogate, were used for tests Lys1 and Lys2. The spores are rod-shaped and the measured size of the *B. subtilis* used was  $0.5 \times 1.5 \mu\text{m}$ . *B. subtilis* is commonly used as a conservative surrogate for *C. parvum* for subsurface transport studies (Bradford et al. 2016), and aerobic spores have been included by the U.S. Environmental Protection Agency as an indicator for *C. parvum* in groundwater under the direct influence (GWUDI) of surface water. Additionally, 1- $\mu\text{m}$  YG carboxyl polystyrene microspheres (Polysciences Inc., Warrington, PA, USA) were injected separately for tests Lys3 and Lys4. The zeta potentials of the *B. subtilis* and the microspheres were measured in order to compare potential attachment differences due to surface charge. For the zeta potential measurements, the water was filtered through 0.20  $\mu\text{m}$  filters before each measurement, and three replicates were done using a Zetasizer Nano ZS (Malvern Panalytical, Worcestershire, UK). The background matrix used was the same as that used during the flow-through lysimeter experiments, which was tap water from the town of Petzenkirchen, Austria (pH of 7.8

and an electrical conductivity of 550  $\mu\text{S}/\text{cm}$ ). Enumeration of *B. subtilis* was done by the pour plate cultivation method (Plate Count Agar, ArtNr. 1.05463.0000, Merck, Germany; incubation  $36 \pm 2$  °C,  $44 \pm 4$  h) and enumeration of microspheres was done with solid-phase cytometry using a *Chem-Scan* RDI (bioMérieux, Marcy l'Étoile, France), following the method outlined in (Stevenson et al. 2014).

### Large-column experimental procedure

Five tracer tests were performed on a saturated 4-m-high (0.78 m in diameter) column of undisturbed (not repacked) gravel material (porous media details in Table 1).

A detailed description of the column installation can be found in (Stevenson et al. 2021a, b). In short, two 2-m high sections were extracted in situ from a gravel pit in central Austria and transported to a laboratory in Petzenkirchen, Austria. The two 2-m sections were fitted together to create an undisturbed 4-m-high gravel column. A video of the installation process is provided in Stevenson (2021b). The lysimeter (large 4-m column) is pictured in Fig. 1b. The small-column test set-up is shown in Fig. 1a, and the field site in Fig. 1c.

**Table 1** Lysimeter material characterization: porosity,  $D_{10}$  and  $D_{50}$  (grain sizes at which 10% and 50% of material passes, respectively)

Material	Depth (cm)	Porosity (-)	$D_{10}$ (mm)	$D_{50}$ (mm)
1	0 - 75	0.11	0.2	8.5
2	75 - 220	0.18	0.8	8.6
3	220 - 245	0.18	0.6	8.0
4	245 - 400	0.11	0.6	6.4

The entire column, or indoor lysimeter installation, is housed in a cool room, allowing the column to be kept at a temperature typical of groundwater, 11–12 °C. Ceramic cup tensiometers (UMS GmbH, Munich, Germany) were installed for taking samples along the length of the 4-m column, but only the lowest sampling point at 3.6-m depth was used for the current analysis, since the other sampling points did not have a difference of scale of one order of magnitude with the small column and field site, which is the focus of this study. Ceramic candles, which are appropriate for collecting *E. coli* and phages (Florent 2022) have a pore size of 20  $\mu\text{m}$ , which is suitable for sampling the colloids used in this study. The method assumes that the volume of the sample removed from each sampling point (100 ml) every 10 min is minimal compared to the total flow volume (one pore volume  $\sim 500$  l) and does not affect the results. Flow-through experiments from the top of the column to the bottom were run using tap water from the town of Petzenkirchen, Austria, as this is representative of the groundwater in the area from which the lysimeter material was taken. The column was initially filled slowly from the bottom up over a period of approximately 24 h to ensure that the air in the column could escape freely to the atmosphere. After reaching a water level of about 2.5 cm above the porous media surface, the filling was stopped and the valve at the bottom was opened, while water was applied at the surface to keep the water level constant. Once a constant flow rate was established, the column was rinsed for 1 day under these conditions before tracer application. Before each test, samples were taken to confirm that there were no colloids from previous experiments still coming through. The tracers were added to the column by pouring the influent pulse on the stable water surface at the top of the saturated lysimeter. This took between 30 s to 1 min, for the small influent volumes used.

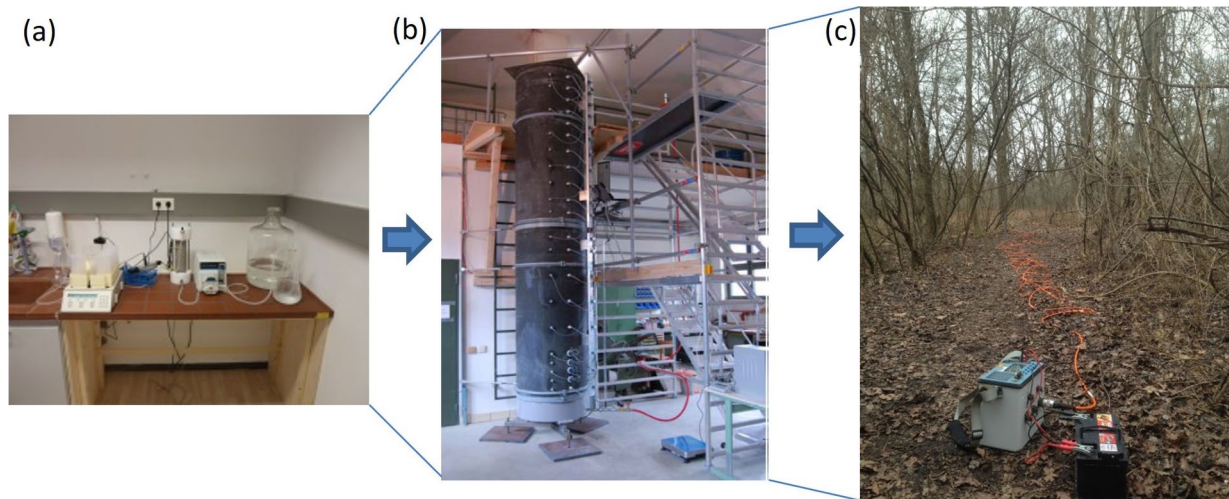


**Fig. 1** Schematic of deterministic upscaling concept. Small column (a), meso-scale column (b), and field site (c)

Bromide was measured in the effluent using an ion-selective electrode for  $\text{Br}^-$ . The ion-selective electrode was calibrated and compared to several data points for which bromide was quantified using ion chromatography. Bromide is considered a conservative tracer due to low background concentrations and lack of sorption to aquifer material (Kasnavia et al. 1999). The experimental conditions are summarized in Table 2. After each test, the large column was flushed for several days, to ensure that a minimal number of colloids remained in the column.

### Field and small-column tests

Methods for the current and previous field tests and small-column tests are described in detail in Oudega et al. (2021). The field site is located in the Lobau National Park, south-east of Vienna, Austria, and the small-column tests were done using material from the drilling cores that were saved when installing the piezometers at the site. One field test using 1- $\mu\text{m}$  YG carboxyl microspheres (as described in the section *Colloids*) diluted in a 1-l bottle to  $4.55 \times 10^8$  particles/ml ( $4.55 \times 10^{11}$  particles in total) was done by injecting in a piezometer that was 25 m from the pumping well. In previous studies by Oudega et al. (2021), *B. subtilis* were injected in a higher amount ( $\sim 10^{12}$  in total) but that amount was cost-prohibitive with commercially available microspheres.

For the current study, three small 50-cm column tests were done using repacked (disturbed) aquifer material and injecting 1- $\mu\text{m}$  YG carboxyl microspheres (described in *Colloids*). Two tests were done using material from the Lobau site, taken at a depth of 11 m from the gravel aquifer (Col3 and Col4), and one test with aquifer material taken at a depth of 3 m, from the site where the lysimeter material was taken

(Col5). Stones larger than 3 cm were removed because the column was only 7 cm in diameter. The aquifer material was undisturbed in the 4-m-high lysimeter, and larger stones were therefore not removed. The small-column tests used fresh aquifer material for each test, whereas the lysimeter was only flushed between tests (i.e., the aquifer material was not changed).

### Data analysis

#### Calculation of log-removal rate

The log-removal rate for a pulse input is calculated using the following formula (Kretzschmar et al. 1997):

$$\lambda = \frac{\ln\left(\frac{Q}{N_0} \int_0^{t_f} C(t) dt\right)}{x} \quad (1)$$

where  $Q$  is the flow rate [ $\text{L}^3/\text{T}$ ],  $N_0$  is the total amount of tracer injected [ $\text{M}$ ],  $C(t)$  is the concentration at time,  $t$ , after injection [ $\text{M}/\text{L}^3$ ],  $t_f$  is the final time of the test after the pulse has passed through [ $\text{T}$ ], and  $x$  is the distance from the injection point to the sampling point [ $\text{L}$ ] ( $\text{M}$ ,  $\text{L}$  and  $\text{T}$  represent mass, length and time units, respectively). A constant log-removal per distance can be used to determine the required setback distance for protection of a drinking water well (Blaschke et al. 2016).

### Numerical modeling

Modeling with the advection–dispersion equation was done with a one-site attachment model and a colloid filtration theory (CFT) model, using HYDRUS (Simunek et al. 2013), which solves the Richards equation for flow in the saturated and

**Table 2** Summary of lysimeter experiments using *B. subtilis* spores and microspheres and additional microsphere experiments in the small column and field

Test	Tracers	Measured flow rate (m/day)	Porosity (-)	Colloidal pulse volume (l)	Bromide mass (g)	Number of colloids	Influent concentration of colloids (particles/ml)
Col3	1- $\mu\text{m}$ spheres/NaBr	9.95	0.22	0.4	0.04	2.51E10	6.27E7
Col4	1- $\mu\text{m}$ spheres/NaBr	6.73	0.17	0.8	0.08	3.90E9	4.88E6
Col5	1- $\mu\text{m}$ spheres/NaBr	6.81	0.24	1	0.1	4.19E9	4.19E6
Fld3	1- $\mu\text{m}$ spheres/NaBr	14	0.12	1	100	4.55E11	4.55E8
Pre	KBr	8.21	0.18	30	30	-	-
Lys1	<i>B. subtilis</i> /KBr	9.04	0.18	1.5	1.5	2.75E11	1.83E8
Lys2	<i>B. subtilis</i> /KBr	8.44	0.18	2.0	4	9.20E10	4.60E7
Lys3	1- $\mu\text{m}$ spheres/NaBr	8.14	0.18	2.0	4	6.05E11	3.03E8
Lys4	1- $\mu\text{m}$ spheres/NaBr	9.04	0.18	1.0	2	5.26E11	5.26E8

*Pre* represents a pre-test done with KBr alone. Col1, Col2, Fld1, and Fld2 are not listed because the results of these tests were published in Oudega et al. (2021)

unsaturated zones. The one-site attachment transport model implemented in HYDRUS follows the theory for kinetically sorbing solute outlined by Cameron and Klute (1977). For the models in the current work, the 1-D and 2-D equations were used (2-D shown here, also applicable to transport in the field-scale model):

$$\frac{\delta c}{\delta t} = D_x \frac{\delta^2 c}{\delta x^2} + D_y \frac{\delta^2 c}{\delta y^2} - \mathbf{v} \frac{\delta c}{\delta x} - \frac{\rho_b \delta S}{\theta \delta t} \quad (2)$$

$$\frac{\rho_b \delta S}{\theta \delta t} = k_{\text{att}} c - \frac{\rho_b}{\theta} k_{\text{det}} S \quad (3)$$

where  $c$  represents the concentration of mobile colloids [M/L<sup>3</sup>],  $D$  is dispersivity [L] (in the  $x$ , and  $y$  directions),  $\mathbf{v}$  is the pore water velocity [L/T],  $\rho_b$  is the bulk density [M/L<sup>3</sup>],  $S$  is the concentration of sorbed colloids [M/M],  $\theta$  is the volumetric water content for this saturated system [-], and  $k_{\text{att}}$  and  $k_{\text{det}}$  are attachment and detachment rate coefficients [1/T], respectively.

The CFT attachment rate coefficient,  $k_{\text{att}}$ , was modeled following the equation from (Tufenkji and Elimelech 2004):

$$k_{\text{att}} = \frac{3(1 - \theta)}{2d} \alpha \eta_o \mathbf{v} \quad (4)$$

Here  $d$  is the representative grain size diameter [L] (normally  $d_{50}$  is used),  $\alpha$  [-] is the attachment efficiency, and  $\eta_o$  [-] is the single-collector contact efficiency. The small column was modeled in 1-D, while the 4-m-high column was modeled in 2-D using 15,600 elements. Constant-head boundary conditions were applied at each end of the column (to represent the stable free surface at 4 m at the top and 0 m at the bottom), with a homogeneous hydraulic conductivity. The initial head conditions were also set to 4 m at the top of the column, 0 m at the bottom, and linearly interpolated between the top and bottom. A 2-D model was used for the lysimeter experiments to allow more degrees of freedom (Fiori and Jankovic 2012). A 3-D equilibrium flow model with homogeneous hydraulic conductivity was employed for the field experiments (the dual permeability module in Hydrus is not available in 3-D).

The value of  $k_{\text{att}}$  in Eqs. (3) and (4) assumes a constant rate of removal. A depth-dependent straining coefficient was employed in Eq. (3) in order to account for non-exponential removal. In this case, the value of  $k_{\text{att}}$  in Eq. (3) was multiplied by an artificial depth-dependent straining function,  $\psi_{\text{str}}$  (artificial because the goal was not to account for straining, but rather non-exponential removal) given as (Bradford et al. 2003):

$$\psi_{\text{str}} = \left( \frac{d_{50} + x}{d_{50}} \right)^{-\beta} \quad (5)$$

where  $d_{50}$  [L] is the median grain size (in the case of this study,  $d_{10}$  was used due to reasons that will be mentioned in the section *Colloid filtration theory equilibrium flow model*), and  $\beta$  is an empirically fitted parameter with a recommended value of 0.43 (Bradford et al. 2003).

Although Eq. (5) is normally used when retention profile information is available, one intention of this study was to test the hypothesis that colloidal removal follows a power law function. Fractal relationships are often used in hydrological systems (Schiavo et al. 2022; Tarboton et al. 1989). A fractal form of the attachment rate coefficient could be written as:

$$k_{\text{att}}(x) = \psi^{-\beta} \cdot k_{\text{att}}(\psi \cdot x) \quad (6)$$

where  $\psi$  represents a ratio of the large scale to the small scale (e.g.,  $(d_{50} + x)/d_{50}$  in the depth-dependent straining function),  $\beta$  is an empirical fitted parameter, and  $x$  is the travel distance (or scale) from inlet to outlet or sampling point, regardless of the path traveled. Other studies use this fractal (power law) relationship to correlate, for example, hydraulic conductivity and porosity (Hergarten et al. 2014), or the emergence of increasing solute concentration organization within preferential flow pathways with increasing variance in hydraulic conductivity (Edery et al. 2014).

A 1-D homogeneous dual permeability model was also used to account for physical non-equilibrium flow in the lysimeter experiments. This model employs advection–dispersion equations in regions of faster (subscript  $f$ ) and slower (subscript  $m$ ) flow (Gerke and Vangenuchten 1993):

$$\frac{\delta c_f}{\delta t} = D_f \frac{\delta^2 c_f}{\delta x^2} - \mathbf{v}_f \frac{\delta c_f}{\delta x} - \frac{\rho_b \delta S_f}{\theta_f \delta t} - \frac{\Gamma_s}{\theta_f w} \quad (7)$$

$$\frac{\delta c_m}{\delta t} = D_m \frac{\delta^2 c_m}{\delta x^2} - \mathbf{v}_m \frac{\delta c_m}{\delta x} - \frac{\rho_b \delta S_m}{\theta_m \delta t} - \frac{\Gamma_s}{\theta_m (1 - w)} \quad (8)$$

$$\Gamma_s = \omega(1 - w)\theta_m(c_f - c_m) + \Gamma_w c^\# \quad (9)$$

The mass transfer coefficient,  $\Gamma_s$  [M/(L<sup>3</sup>·T)], allows for exchange between the fast and slow flow zones,  $\Gamma_w$  is a water transfer term [1/T],  $w$  [-] represents the fraction of the porous media with fast flow ( $0 < w < 1$ ), and  $\omega$  [1/T] is a first-order diffusive mass transfer coefficient. For values of  $\Gamma_w > 0$ ,  $c^\#$  is equal to  $c_m$  and for  $\Gamma_w < 0$ ,  $c^\#$  is equal to  $c_f$ . In the dual permeability model, the attachment rate is accounted for with a first-order sink term. That is,  $\frac{\rho_b \delta S}{\theta \delta t}$ , defined in Eq. (3), is represented with subscripts  $f$  and  $m$  for fast and slow zones, Eqs. (7) and (8), respectively. The boundary conditions used to solve the equations were a constant head boundary condition at the top of the column, with the concentration of the influent, and a zero gradient at the bottom of the column.

## Moments of the breakthrough curves

In order to investigate the extent of heterogeneity in the porous media, the moments of the breakthrough curves were estimated according to the following formulas (Riva et al. 2008):

$$T_1 = \frac{\int_0^\infty tc(t)dt}{\int_0^\infty c(t)dt} \quad (10)$$

$$\tau_2 = \frac{\int_0^\infty [t - T_1]^2 c(t)dt}{\int_0^\infty c(t)dt} \quad (11)$$

$$C_s = \frac{\int_0^\infty [t - T_1]^3 c(t)dt}{\left[ \int_0^\infty [t - T_1]^2 c(t)dt \right]^{3/2}} \left[ \int_0^\infty c(t)dt \right]^{1/2} \quad (12)$$

$T_1$  [T] is the first moment and represents the mean arrival time of the center of mass of the tracer.  $\tau_2$  [T<sup>2</sup>] is the second moment and is related to the spreading or dispersion of the tracer, and  $C_s$  [-] is an indication of the skewness or asymmetry of the breakthrough curve (higher skewness indicates a higher degree of heterogeneity).

## Results

The zeta potentials of the colloids used in the experiments were similar in the background matrix, which was filtered Petzenkirchen tap water. *B. subtilis*, suspended in the background matrix, had a zeta potential of  $-22.42 \text{ mV} \pm 0.67$ , the 1- $\mu\text{m}$  microspheres had a zeta potential of  $-24.72 \text{ mV} \pm 0.70$ . In the column test 4 (Col4), the zeta potential and size of the microspheres were measured in the influent at the beginning of injection and at the end, as well as in the effluent, to see if there was preferential attachment of microspheres. It was found that the zeta potential and size of the colloids were stable in the influent and effluent solutions, indicating a lack of attachment due to heterogeneity amongst the colloids (i.e., surface charge and size). Additionally, Col4 was excavated and 98% of the colloids were recovered either in the effluent or from the porous media. This was done in order to demonstrate that an accurate mass balance could be achieved according to the methods used for the small-column tests. For the lysimeter tests, it was not possible to excavate the column. In the field, *B. subtilis* were detected at a travel distance of 25 m, by taking samples from the pumping well, but not the 1- $\mu\text{m}$  microspheres. As previously stated, a lower number of microspheres were injected in the field due to cost constraints (i.e.,  $1.65 \times 10^{12}$  and  $1.16$

$\times 10^{12}$  *B. subtilis* were injected in total for tests Fld1 and Fld2 (Oudega et al. 2021), versus  $4.55 \times 10^{11}$  microspheres in total for Fld3). Therefore, a second injection test using microspheres in the field was not done.

As the focus of this paper is the meso-scale, only the modeling results for the lysimeter are shown here (1-site kinetic equilibrium flow model, Fig. 2). The transport at 3.6 m depth was comparable for the 1- $\mu\text{m}$  microspheres and *B. subtilis*, both of which not only had a similar zeta potential but also analogous sizes.

After fitting, by trial-and-error, the 2-D numerical model of the lysimeter to the bromide breakthrough curves by adjusting the flow velocity (listed in Table 5), dispersivity and porosity for Materials 1–4 (materials listed in Table 1), these values were used to model the colloidal breakthrough curves. In Fig. 2, it is visually apparent that the colloidal transport experiments are in heterogeneous material because the breakthrough curves of the colloids arrive before the bromide curve, and the bromide curve is very asymmetrical, with heavy tailing, which indicates preferential flow (Fogg and Zhang 2016). Also, quantitatively (see Table 3), the skewness coefficients for the breakthrough of bromide in all experiments were above +1, indicating a heavier front to the left of the curve with tailing towards the right. The highest values for the skewness coefficient were calculated for the lysimeter data, suggesting that the porous media in the lysimeter is more heterogeneous than the Lobau material in the field and in the small columns. In the case of the small columns, this may be because large stones had to be removed for practical reasons.

The porosity values (measured for small columns gravimetrically and otherwise estimated before calibration) for all the experiments are shown in Table 2, as well as the measured flow rates. The dispersivity in the lysimeter tests was found to be 30 cm for bromide and 21 cm for both types of colloids in all test runs, using the equilibrium flow model. Dispersivity of microbes and other colloids is less than for conservative solute tracers due to colloidal transport being constrained to coarser flow paths (Grindrod et al. 1996; Pang et al. 2008). In regards to the question of flow rate, the small columns were run between 6.72 and 9.95 m/day, the lysimeter between 8.14 and 9.04 m/day, and the field tests were run at three different flow rates: 2, 14, and 24 m/day (Oudega et al. 2022); however, the comparison in this paper is with the  $\sim 14$  m/day results (Oudega et al. 2021), as this flow rate was closest to the flow rate of the lysimeter tests.

## Colloidal removal

Table 4 shows the results for the log-removal rate calculations, according to Eq. (1), and the moment analysis. Results are similar for the spores (tests Lys1 and Lys2) and microspheres (tests Lys3 and Lys4).

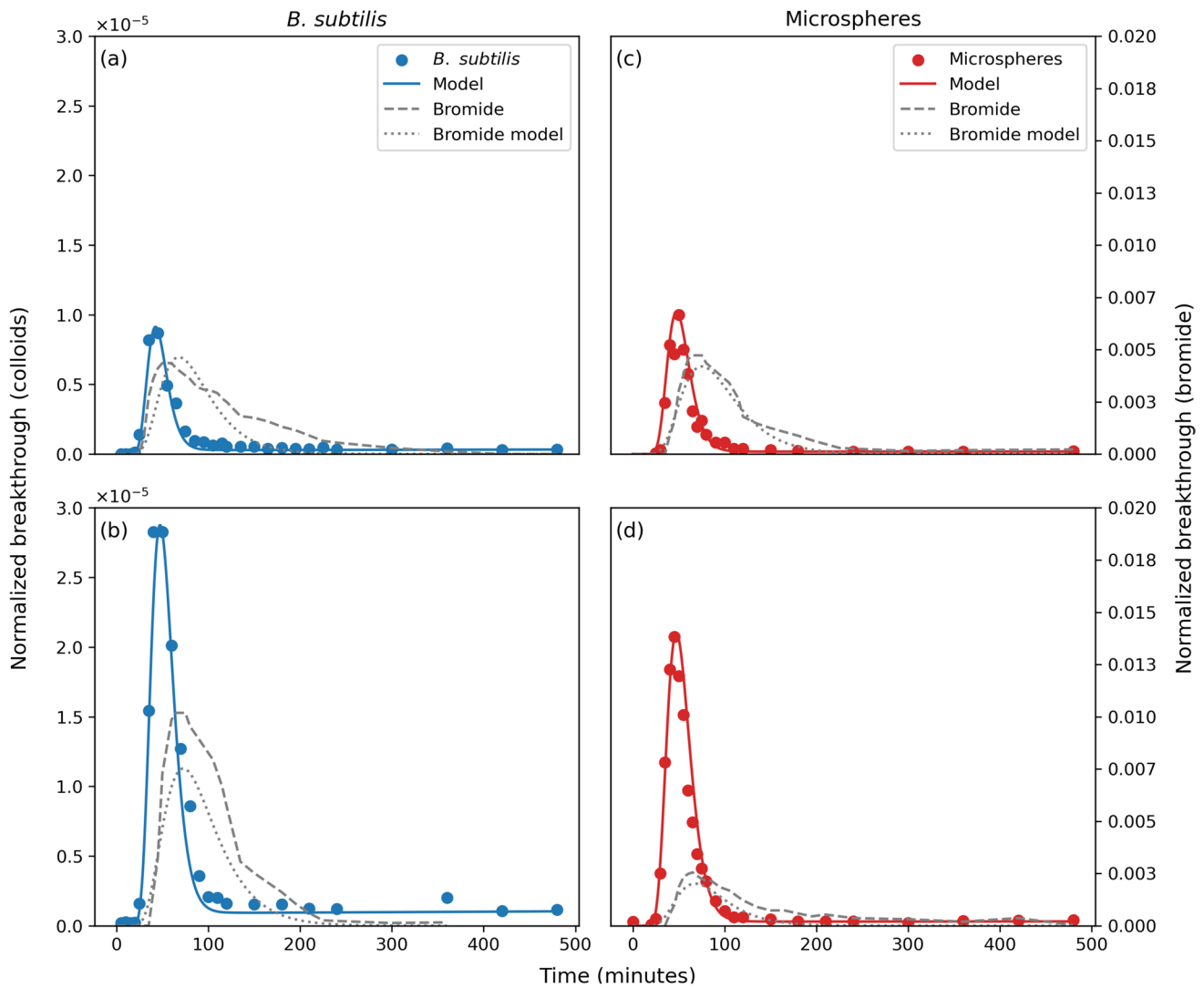


**Fig. 2** Breakthrough curves of *B. subtilis* (plot **a** is test Lys1, and plot **b** is test Lys2) and 1- $\mu\text{m}$  microspheres (plot **c** is test Lys3, and plot **d** is test Lys4) in the lysimeter (the measured bromide data are the

dashed grey lines and *B. subtilis* spores are the blue scattered data points while microspheres are red). The modeled lines are from the Hydrus 2-D equilibrium flow model

The average log-removal for *B. subtilis* in the two lysimeter tests is 1.73 log/m. The log-removal rates of *B. subtilis* in the field were the same order of magnitude for all the flow rates tested in Oudega et al. (2022) (0.19–0.28 log/m). For the current study, the log-removal rates in the field for the middle flow rate (14 m/day) were used for comparison (i.e., 0.22 log/m on average) since the flow was closest to the flow rates in the small columns and the lysimeter. In the small-column tests from Oudega et al. (2021), the average log-removal for *B. subtilis* was 19.38 log/m. Therefore, for a difference of one order of magnitude for each measurement scale (0.1, 1 and 10 m), the log-removal rate is approximately 20, 2, and 0.2 log/m, respectively. The product of each being 2 (i.e.,  $0.1 \times 20$ ,  $1 \times 2$ ,  $10 \times 0.2$ ) means that they have an inversely proportional relationship. As the study by

Oudega et al. (2021) already found a difference of two orders of magnitude between log-removal at the small column and field scale, the current study with a meso- (intermediate) scale column brings insight and strengthens the hypothesis.

## Numerical modeling

### Attachment–detachment equilibrium flow model

The attachment–detachment model in Hydrus 2-D was used to model the breakthrough curves of the tracers at the 3.6-m depth sampling point in the lysimeter with  $R^2$  values ranging from 0.84 to 0.97 for bromide and from 0.95 to 0.98 for the colloids (Table 5). Comparing the  $K_{\text{att}}$  values to those in the small columns and field also found an order of magnitude

**Table 3** Calculated 1st moment, 2nd moment, and skewness coefficient for bromide experiments

Scale (m)	Test	Tracer	$T_1$ (h)	$\tau_2$ (hr <sup>2</sup> )	$C_s$ (-)
0.1	Col1	<i>B. subtilis</i>	0.77	0.66	1.14
	Col2	<i>B. subtilis</i>	0.79	0.69	1.16
	Col3	1- $\mu$ m spheres	0.51	0.30	1.29
	Col4	1- $\mu$ m spheres	0.76	0.64	1.13
	Col5	1- $\mu$ m spheres	0.73	0.64	1.23
1	Lys1	<i>B. subtilis</i>	2.11	6.23	1.53
	Lys2	<i>B. subtilis</i>	1.80	4.05	1.41
	Lys3	1- $\mu$ m spheres	2.30	8.35	1.85
	Lys4	1- $\mu$ m spheres	2.86	12.38	1.59
10	Fld1	<i>B. subtilis</i>	13.58	215.04	1.22
	Fld2	<i>B. subtilis</i>	11.42	142.00	1.13

pattern, shown in Table 5 and also in Fig. 3, on a log–log plot. Table 5 illustrates how the  $K_{att}$  value can be increased, almost to the value of the small columns, by introducing a depth-dependent straining function,  $\psi_{str}$  (which is multiplied by  $K_{att}$  in Eq. (3)). In this way, small-column tests could be run, using a pathogen, and the  $K_{att}$  from the small scale could be used in a model at the meter scale, by using a similar depth-dependent function (even if there is no straining) when field-scale tracer test data are not available. As the field tests were modeled in 3-D, it was not possible to use the depth-dependent straining function, which is not available in Hydrus 3-D.

**Colloid filtration theory equilibrium flow model**

For the modeling done with CFT (Eq. 4),  $d_{10}$  was used instead of  $d_{50}$  (listed in Table 1) because the finer material is more important for colloidal removal in heterogeneous

porous media (Pang et al. 2005). Martin et al. (1996) found that  $\alpha$  decreases with travel distance in different-sized porous media, and concluded that using  $d_{10}$  as the representative grain size diameter gives the best match to the data.

For the small column and field material (Lobau National Park), the  $d_{10}$  was 0.150 mm and for the lysimeter it was 0.520 mm, on average. Additionally, one small-column test (Col5) was run using material taken from the same site as the lysimeter, but the material had a  $d_{50}$  of 3.92 mm, and the  $d_{10}$  was 0.03 mm, which was less similar to the lysimeter than the Lobau material. This had an impact on  $\eta$  and  $\alpha$ , however, one can still see the order of magnitude pattern on a log–log plot (Fig. 3c), with the data point from Col5 being the outlier. The value,  $\eta$ , is the single-collector removal efficiency (Tufenkji and Elimelech 2004) and represents the rate at which suspended particles or colloids making contact with a grain of aquifer material leads to attachment. This is not to be confused with  $\eta_o$ , the rate that they strike the collector. In the current study,  $\eta$  is considered to be the actual single-collector removal efficiency, which is lower than  $\eta_o$ , the single-collector contact efficiency (Tufenkji and Elimelech 2004), and  $\alpha$ , the empirical attachment (collision) efficiency, where  $\alpha = \eta/\eta_o$ , the ratio of the rate that particles stick to the rate they strike the collector (Logan et al. 1995).

Figure 3 shows graphs over three orders of magnitude for travel distance versus three orders of magnitude of log-removal, attachment rate, and CFT removal efficiency. The blue data points can be compared directly, since these points represent the same microorganism (*B. subtilis*). The red points are bacteriophages  $\phi X174$ , with a diameter of 26 nm, (used in the field and small columns (Oudega et al. 2021)) and 1- $\mu$ m microspheres (used in the small columns and in the lysimeter). With this graphic, it is intended to illustrate how the removal of colloids can be categorized according to the scale on which the data were measured, and that on a log–log plot, the data (being linear) follow

**Table 4** Calculated log-removal, 1st moment, 2nd moment and skewness coefficient for colloidal experiments

Scale (m)	Test	Tracer	Removal, $\lambda$ (log/m)	$T_1$ (h)	$\tau_2$ (hr <sup>2</sup> )	$C_s$ (-)
0.1	Col1	<i>B. subtilis</i>	18.55 <sup>a</sup>	3.69	16.15	1.20
	Col2	<i>B. subtilis</i>	20.20 <sup>a</sup>	2.76	9.98	1.40
	Col3	1- $\mu$ m spheres	15.83	2.50	15.30	1.80
	Col4	1- $\mu$ m spheres	27.10	3.89	17.20	1.13
	Col5	1- $\mu$ m spheres	3.98	0.64	0.50	1.23
1	Lys1	<i>B. subtilis</i>	1.95	2.22	9.78	1.92
	Lys2	<i>B. subtilis</i>	1.50	2.45	11.45	1.81
	Lys3	1- $\mu$ m spheres	1.94	1.91	7.32	2.18
	Lys4	1- $\mu$ m spheres	1.69	1.66	6.12	2.38
10	Fld1	<i>B. subtilis</i>	0.23 <sup>a</sup>	14.25	292.54	1.37
	Fld2	<i>B. subtilis</i>	0.21 <sup>a</sup>	10.23	131.41	1.35

<sup>a</sup>Data taken from (Oudega et al. 2021)

**Table 5** Equilibrium flow model results

Scale (m)	Test	Calibrated flow rate (m/day)	$K_{att}$ (1/h)	$K_{att}^*$ (1/h)	$K_{att}^{**}$ (1/h)	$K_{det}$ (1/h)	Bromide $R^2$	Colloid <sup>b</sup> $R^2$	$\eta_0$	$\alpha$	$\eta = \eta_0 \cdot \alpha$
0.1	Col1 <sup>a</sup>	6.72	50.77	-	-	0.048	-	-	3.99E-2	1.01E-1	4.05E-3
	Col2 <sup>a</sup>	6.72	117.82	-	-	0.059	-	-	3.98E-2	1.86E-1	7.41E-3
	Col3	9.95	50.40	-	-	0.018	-	-	2.09E-2	7.80E-2	1.63E-3
	Col4	6.77	57.00	-	-	0.018	-	-	2.48E-2	1.75E-1	4.34E-3
	Col5	8.21	13.20	-	-	0.018	-	-	1.55E-1	3.30E-4	5.12E-5
1	Lys1	9.07	7.20	25.2	23.4	0.012	0.84	0.97	9.04E-3	3.10E-2	2.80E-4
	Lys2	8.50	5.88	20.4	18.6	0.012	0.97	0.98	9.37E-3	2.50E-2	2.34E-4
	Lys3	8.21	6.24	21.6	19.8	0.006	0.97	0.95	9.75E-3	2.70E-2	2.63E-4
	Lys4	9.07	4.95	16.2	15.0	0.006	0.91	0.97	9.23E-3	2.00E-2	1.85E-4
10	Fld1 <sup>a</sup>	14.75	0.95	N/A	N/A	0.004	-	-	5.70E-2	5.95E-4	3.39E-5
	Fld2 <sup>a</sup>	13.36	1.01	N/A	N/A	0.003	-	-	5.87E-2	4.09E-4	2.40E-5

N/A not applicable in 3-D model

$\eta_0$ ,  $\alpha$  and  $\eta$  according to (Tufenkji and Elimelech 2004)

<sup>a</sup>Data taken from (Oudega et al. 2021)

<sup>b</sup> $R^2$  value for 1-site kinetic model without straining factor

\*with depth-dependent straining function,  $\beta = 0.9$

\*\*with depth-dependent straining function,  $\beta = 0.43$  as per (Bradford et al. 2003)

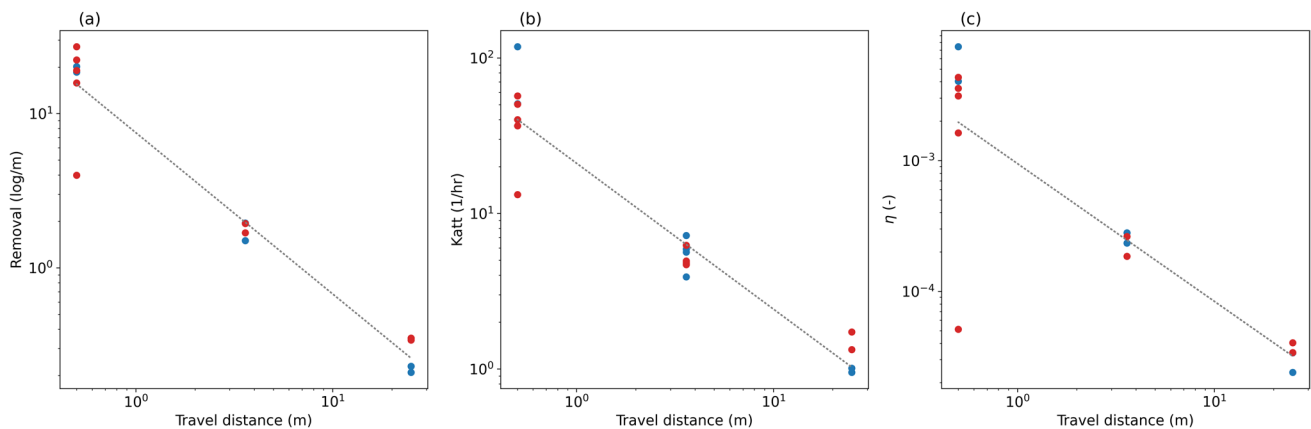


**Fig. 3** Removal (a), attachment rate (b), and colloid filtration theory removal efficiency (c) plotted against travel distance for the small laboratory columns, a large intact core and a real-world gravel aquifer. Blue dots are data points for *B. subtilis*, for direct comparison, and the red dots are other (phages and microspheres). The data for the phages and *B. subtilis* in the small columns and field experiments were taken

from (Oudega et al. 2021). All parameters exhibit a power law, i.e., linear on log–log plot, regardless of colloid type. The attachment rate graph (b) contains results from the equilibrium and dual permeability flow models. Take note that the CFT modeling results do not take dual permeability into account

the power law. For this study, the focus is the order of magnitude only, and from this perspective, one can see that the type of colloid is not as important. It is often hypothesized that at smaller colloid sizes (i.e., < 100 nm), colloid characteristics and chemical conditions are more dominant than scale effects (Lin et al. 2022). The results of this study show that over orders of magnitude, regardless of colloid population or size, a fractal pattern of colloid removal develops.

### Dual permeability non-equilibrium flow model

Additionally, the lysimeter was modeled in Hydrus 1-D using the dual permeability model, in order to allow for the influence of preferential flow. Figure 4 shows the modeling results as well as Table 6. The  $K_{att}$  values are slightly lower than for the equilibrium flow model, but on the same order of magnitude, as is apparent in Fig. 3, which also contains the dual permeability  $K_{att}$  results.

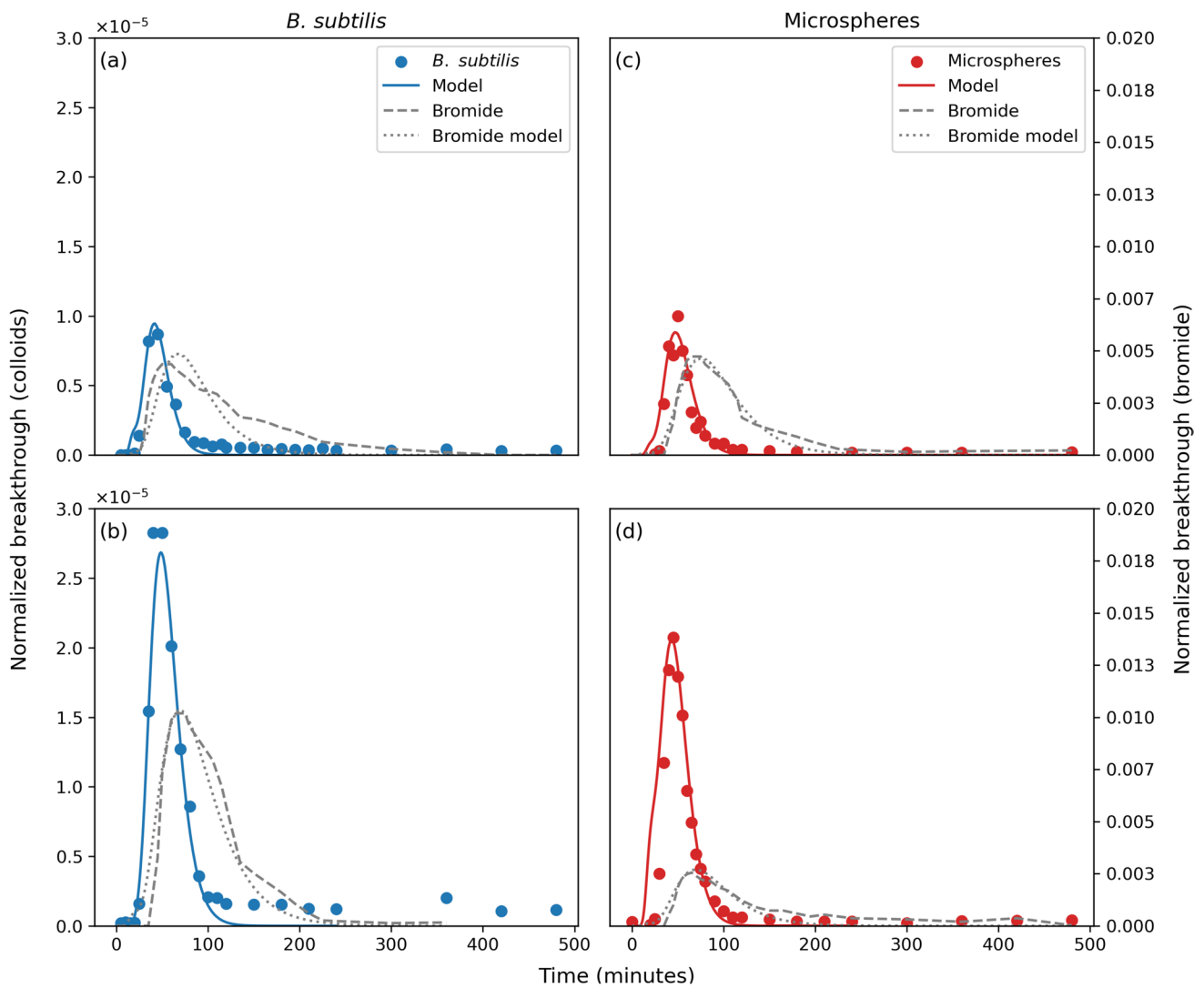


**Fig. 4** Breakthrough curves of *B. subtilis* (plot (a) is test Lys1, and plot (b) is test Lys2) and 1- $\mu$ m microspheres (plot (c) is test Lys3, and plot (d) is test Lys4) in the lysimeter (the measured bromide data

are the dashed grey line and *B. subtilis* spores are the blue scattered data points while microspheres are red). The modeled line is from the Hydrus 1-D dual permeability model

In Figs. 2 and 4, it is visually apparent that the bromide data sets were modeled better with the dual permeability model, but the colloids were modeled slightly better with the equilibrium flow model. This is also reflected by the  $R^2$  values. The improved modeling of the bromide breakthrough curve using a dual permeability model may be due to the bromide accessing the fast and slow zones, whereas the colloids may only access one flow zone because of size exclusion.

## Discussion

### Power law relationship

The original plan for this project was to inject tracers in other observation wells, the furthest being approximately 100 m from the pumping well. However, since the

**Table 6** Dual permeability non-equilibrium model results

Test	Cali- brated flow rate (m/day)	$w$ (-)	$v_m$ (m/day)	$v_f$ (m/day)	Bromide model				Colloid model				$\omega$ (1/h)	$K_{att}$ (1/h)	Bromide $R^2$	Colloid $R^2$
					$\theta_m$	$\theta_f$	$D_m$ (cm)	$D_f$ (cm)	$\theta_m$	$\theta_f$	$D_m$ (cm)	$D_f$ (cm)				
Lys1	9.14	0.15	7.77	1.37	0.2	0.3	45	45	0.2	0.3	40	20	0.0003	5.64	0.86	0.96
Lys2	8.46	0.15	7.19	1.27	0.2	0.3	45	45	0.2	0.3	40	20	0.0003	3.90	0.97	0.97
Lys3	7.78	0.15	6.61	1.17	0.2	0.3	45	45	0.2	0.3	40	20	0.0003	4.80	0.97	0.92
Lys4	8.80	0.15	7.48	1.32	0.2	0.3	45	45	0.2	0.3	40	20	0.0003	4.68	0.92	0.95

breakthrough of colloids was already very low at the point where samples were taken for the initial field tests (25-m travel distance), it was not even attempted. This points to the main issue that the scale at which it is possible to detect colloids does not correspond to the scale at which data are required in order to be representative. Redman et al. (2001) alludes to an REV with a filtration length scale and proposes modeling CFT with a power law function based on a particle filtration distribution that depends on scale-free or fractal phenomena (power law); however, their filtration length scale depends on the scale of measurement, which goes back to the original conundrum.

The power law phenomenon has been previously linked to dispersivity, which increases as the transport scale increases (Wheatcraft and Tyler 1988). Neuman (1990) also investigated dispersivity, as well as hydraulic conductivity, and how the relationship with scale follows a power law (or fractal scaling) and appears to be independent of porous media, i.e., the effect is observed for porous and fractured media. Bloeschl and Sivapalan (1995) also discuss the applications of fractals in hydrology and the power law is used to analyze concentration-discharge relationships for surface water runoff (Wymore et al. 2023). Until now, groundwater flow has been treated differently than surface water runoff models, while the processes and transport mechanisms may be similar (Berkowitz and Zehe 2020), especially in heterogeneous, unconfined aquifers, such as alluvial aquifers, which are often used as a drinking water resource via bank filtration. The time of concentration in surface water is actually the opposite for groundwater, which could be called the time of de-concentration, or dispersal.

Log-removal assumes a constant removal rate regardless of distance traveled, although this is not what is observed in experiments at different scales (Oudega et al. 2021). This illustrates how deterministic scaling methods may be useful in upscaling log-removal from the smaller measurement scale to the larger scale of practical application. Interestingly, the log-removal graph could be extended to 87 m (for *B. subtilis* 3.12E-2 log/m) and 920 m (*B. stearothermophilus* 3.40E-3 log/m), both measured in a coarse gravel aquifer (Pang 2009), with points falling on the same order of magnitude line (linear on log–log plot, Fig. 5).

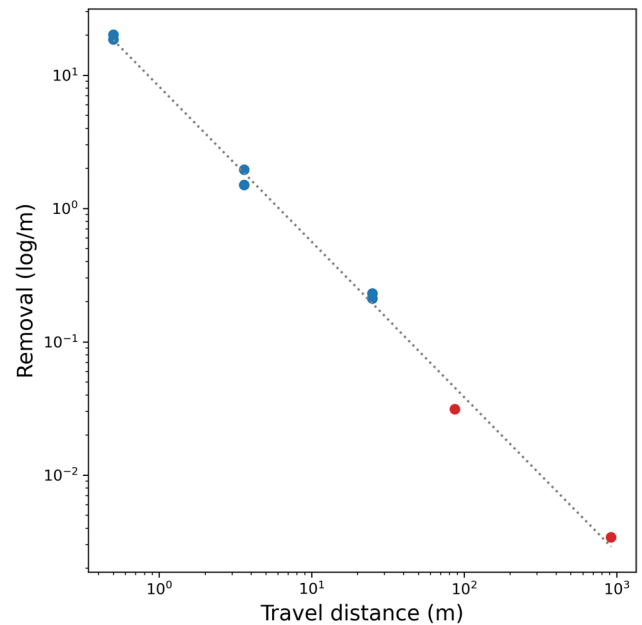


**Fig. 5** Log-removal rates (calculated as log/m) of *B. subtilis* and *B. stearothermophilus* versus travel distance in various heterogeneous materials. Only these microorganisms are shown in order to make the comparison as direct as possible. The *B. subtilis* data from this study and Oudega et al. (2021) are shown in blue, as well as red data points taken from Pang (2009) for *B. subtilis* and *B. stearothermophilus* at travel distances of 87 and 920 m, respectively. This graph allows colloidal log-removal to be compared over five orders of magnitude

This has implications for colloidal transport modeling using a constant attachment rate because it is apparent that this parameter is also dependent on scale and decreases with distance according to the power law. This non-linear effect of  $K_{att}$  was alluded to in Schijven et al. (2002b), where they found that it was necessary to have two kinetic sites, a  $K_{att1}$  and  $K_{att2}$  (a fast attachment site and a slow one) because  $K_{att}$  is not constant.

One way to change the attachment–detachment equation so that the  $K_{att}$  follows a power law, is by multiplying  $K_{att}$  by the depth (or transport distance)-dependent straining coefficient (Bradford et al. 2003). The original meaning of straining by Bradford et al. (2003) hypothesizes that the decreasing removal of colloids with distance is due to the

continuous pore network that is available to those colloidal particles that succeed at traveling over a longer distance. Using a traffic analogy, the majority of a tracer mass is lost in the back streets, possibly with dead-end streets and cul-de-sacs, and a smaller portion of the mass finds the highway. The portion of the tracer on the highway becomes trapped in the middle lane or is going so fast that it misses the exit ramps. In the case of colloids, due to size, they would be capable of entering the smaller pores, but they bypass them as they are going too fast and are also less likely to attach electrostatically at higher velocities (Oudega et al. 2022). The tracer mass lost in the back streets may be delayed, like the solutes having a waiting time in the immobile zones (Haggerty et al. 2000; Schumer et al. 2003). In terms of solute transport, one theory as to why the observed tendency towards self-organized preferential flow may happen is that decreasing entropy with distance in the transverse direction occurs due to the second law of thermodynamics and the required amount of work that is needed to go further distances (Zehe et al. 2021).

It should be noted that, using an equilibrium flow model, the small-column tests were modeled in 1-D, the lysimeter tests were modeled in 2-D, and field tests were modeled in 3-D. Due to the degrees of freedom, it is necessary to model preferential flow/heterogeneous material in 3-D (Fiori and Jankovic 2012). The depth-dependent straining function in HYDRUS is available in 1-D and 2-D only. In this study, it was possible to adjust the attachment rate using the depth-dependent straining function,  $\psi_{str}$ , so that the meso-scale lysimeter has an attachment rate that is closer to the attachment rate in the small-column tests, and the straining function used a  $\beta$  value of 0.9 (a  $\beta$  value of 0.43, as suggested in Bradford et al. (2003), produced a lower attachment rate (Table 5)). This was done in order to show that a depth-dependent function (not only for straining) could be used to allow for decreasing removal of colloids with distance, when field data are not available. Alternatively, in an attempt to address the existence of preferential flow, the lysimeter was modeled in 1-D using a dual permeability model that allows for fast and slow areas of flow. Using the dual permeability model, the  $K_{att}$  rates were actually slightly lower and less similar to the small-column-scale rates. Modeling the small columns using a 1-D dual permeability model (data not presented in this paper), increased the  $K_{att}$  rates slightly. Therefore, using the dual permeability model magnified the difference between the  $K_{att}$  rates at different scales. This may be due to the small columns being repacked, causing the fast-flowing zone to be relatively slower than in the undisturbed meso-scale column.

Although it has already been suggested that colloidal removal may exhibit a power law deposition profile after an initial threshold of exponential removal close to the inlet of an experiment, this contradicts the traditional CFT transport

model that is commonly used (Logan et al. 1995; Yao et al. 1971; Matthess et al. 1988). Martin et al. (1996) recommend scaling filtration rates for different transport distances, using a dimensionless collision number. Schijven and Simunek (2002) found that  $\alpha$  decreased at least one order of magnitude, over 10 m of colloidal transport in dune sand, using a 2-D model, while  $\eta_0$  stayed relatively constant. This is similar to the results of the current study, which finds orders of magnitude difference over 25 m for  $\alpha$  (0.1–0.0005), while  $\eta_0$  remained on the same order of magnitude (0.01–0.06). Also in sand, over a 25-m transport distance in laboratory experiments (Lutterodt et al. 2011) found decreasing  $\alpha$  with distance traveled, although not a full order of magnitude from the 6–26 m scale. In a different study, small-column tests (12 cm) using homogeneous sand found decreasing colloidal removal with depth at high ionic strengths of the influent water and the authors derived an ionic strength-dependent power law for CFT (Tiraferrri et al. 2011). Schijven and Simunek (2002) concluded that the relatively small variation in  $\eta_0$  (single collector efficiency), and high variation in  $\alpha$  (collision efficiency) shows that non-linear removal is not due to physical heterogeneity, but rather soil grain–colloid interactions. In the present study,  $\alpha$  and  $\eta$  decrease one order of magnitude for each order of magnitude increase in scale and, one could argue, represents physical heterogeneity, as it would be a rather large coincidence if the pattern of chemical heterogeneity was consistent at the small-column scale, the meso-scale (lysimeter), and also at the field scale.

### The role of preferential flow: what is the physical process?

Pang (2009) suggested that the non-linear microbial removal rate may be due to bacterial population heterogeneity, however, the present work suggests that it is due to physical processes, such as preferential flow. Oudega et al. (2022) hypothesized that as the degree of preferential flow increases, the velocities in these flow paths increases, decreasing travel time (and therefore contact time), which decreases the attachment rate. The missing puzzle piece is long-distance (scale 100 m or greater) colloidal transport in sand, but this is difficult to measure, due to the high removal of colloids in sand. It would appear from data in dune sand (Schijven et al. 1999) that the log-removal of two different bacteriophages (MS2 and PRD1) at a distance of 30 m is also 0.2 log/m (the same as the current study's gravel aquifer site at 25 m) (information taken from Pang (2009)). It was found that the logarithmic reduction of the microorganisms in dune sand was not linear, and it was hypothesized that the higher colloidal removal close to the injection point was due to patches of positive charge because of ferric oxyhydroxides in the first 8 m, which causes higher attachment of negatively charged

colloids (Schijven et al. 2000). Column experiments were also done by the authors to confirm that the reason that more removal of microorganisms was close to the injection point was due to soil chemical heterogeneity (ferric oxyhydroxides) that decreased with distance (Schijven et al. 2002a). It could be that preferential flow paths are also present in relatively homogeneous sand, due to the previously mentioned theory of self-organization, entropy, and work (Zehe et al. 2021). Even artificially homogeneous glass beads showed more removal of microorganisms close to the injection point, which was attributed to population heterogeneity (Tufenkji 2006). The hypothesis of aquifer material heterogeneity and microorganism population heterogeneity could be disproven by testing microspheres in columns of glass beads.

Regardless of population heterogeneity, the type of colloid used, chemical heterogeneity of the porous media, or ionic strength, the research suggests that well capture zones based on a constant log-removal are not reliable without accounting for scale and preferential flow. In the current study, microspheres were used at the small-column scale and the meso-scale, and the power law was still observed, even though commercially produced microspheres should have minimal population heterogeneity (compared to microorganisms). The observed non-linear pattern of removal at different scales seems to hold true in various types of aquifer material, with different water matrices, and using different types of colloids. In terms of oxic conditions being present and the precipitation of, for example, iron causing more removal close to the injection site in the field, the repacked small-column and meso-scale experiments have been exposed to oxygen, were not run under anoxic conditions, and increasing removal with scale was still observed.

The exact mechanism causing this phenomenon is unclear. It may be that the repacking of the small columns, and even the undisturbed gravel column, have disturbed preferential flow paths, artificial clogging areas from the fine material at the outlet and/or fine material lost during flushing. One theory is that where preferential flow paths are present, colloids will find the center of fast flow paths and although, due to size, they could leave the main flow path, the colloids are transported further and faster than the conservative tracer because they choose the easiest flow path. This process would not be as apparent at the small scale, due to re-packing, and because the travel distance is not long enough to demonstrate the effects of momentum. Another theory is self-organization (as mentioned above), which requires time and distance to appear; at the smaller scale this would not be observed. Physically, self-organization may be due to bypass flow that is caused by physical cracks, zones of relatively higher conductivity, or other processes, which are not present at the small-column scale.

## Conclusions

As climate change promotes more climate extremes, such as unexpected flash floods, groundwater may be more at risk for contamination by surface contaminants such as pesticides, microplastics, contaminants of emerging concern, and pathogens. A large amount of water pushing colloids and solutes quickly through preferential flow paths and negatively influencing groundwater quality may be one impact that climate change has on water resources, and extreme rainfall events could exacerbate the risk to human health. This is especially a concern when vectors enhancing contaminant transport (e.g., co-transport of pathogens with microplastics) find a preferential flow path and is critical when, for example, karst is the drinking water source and microplastics can be carried by wind and deposited on isolated areas.

Colloidal transport is helpful for investigating upscaling relationships for preferential flow in porous media. One goal of the current study was to find if similar colloidal attachment coefficients could be used at different scales in similar porous media, by using a power function (such as the depth-dependent straining function) or a dual permeability model at an intermediate scale. It was found that by using a power function, it was possible to increase the attachment coefficient,  $K_{att}$ , so that the meso-scale  $K_{att}$  was closer to the small-scale value. Contrarily, using a dual permeability model increased the difference between attachment rates at the meso- and small-scales, making  $K_{att}$  less similar. The present study suggests that colloidal removal rates, whether it be log-removal, attachment rates, or CFT removal efficiency, are dependent on the measurement scale and should perhaps be a higher-order than first-order equations, since the removal with distance follows a power law rather than an exponential law. This has implications for groundwater transport of emerging contaminants, such as microplastics and PFAS, as long PFAS chains may behave like a colloid. Future research should focus on confirming this hypothesis in other materials and at other sites, and developing new testing protocols (taking measurement scale into account) and modeling methods for predicting contaminant transport, which seems to be highly dependent on preferential flow. We suspect this also holds true for solute transport and the future lies in modeling heterogeneous flow with upscaled pore network models using neural network methods, probabilistic delineation approaches or travel time methods. Stochastic modeling of heterogeneity assumes randomness of a physical process that may not be as random as previously thought. Colloidal transport offers insight about processes that conservative tracers may not elucidate. This work shows that we need to re-evaluate how groundwater testing is done and how this information is incorporated into numerical groundwater models for heterogeneous aquifers.

**Acknowledgements** This research was funded in whole or in part by the Austrian Science Fund (FWF) [10.55776/T970]. For open access purposes, the author has applied a CC BY public copyright license to any author accepted manuscript version arising from this submission. The work was additionally supported by the Vienna Water Resource Systems Project (ViWa 2020 +) with Vienna Waterworks (MA31). The authors would like to thank Andreas H. Farnleitner for help in procuring funding and Scott A. Bradford for his valuable suggestions and review of the manuscript. Gratitude also goes to Rosa Bertl, Ahmad Ameen, Julia Derx, and Monica Riva for their input.

**Author contribution** M.E. Stevenson: Conceptualization, Methodology, Formal analysis, Investigation, Writing – original draft preparation, Visualization, Funding acquisition. T.J. Oudega: Investigation, Writing – review and editing. G. Lindner: Investigation. R. Sommer: Resources, Writing – review and editing. A.K.T. Kirschner: Resources, Writing – review and editing. A. Scheidl: Conceptualization. A. Eder: Project Administration. P. Strauss: Resources. G. Blöschl: Conceptualization, Writing – review and editing. A.P. Blaschke: Conceptualization, Supervision.

**Funding** Open access funding provided by TU Wien (TUW). This research was funded in whole or in part by the Austrian Science Fund (FWF) [10.55776/T970]. For open-access purposes, the author has applied a CC BY public copyright license to any author-accepted manuscript version arising from this submission.

**Availability of data and materials** Data available upon request.

## Declarations

**Ethics approval and consent to participate** NA.

**Consent for publication** The authors give consent for publication.

**Competing interests** The authors declare that they have no conflicts of interest.

**Open Access** This article is licensed under a Creative Commons Attribution 4.0 International License, which permits use, sharing, adaptation, distribution and reproduction in any medium or format, as long as you give appropriate credit to the original author(s) and the source, provide a link to the Creative Commons licence, and indicate if changes were made. The images or other third party material in this article are included in the article's Creative Commons licence, unless indicated otherwise in a credit line to the material. If material is not included in the article's Creative Commons licence and your intended use is not permitted by statutory regulation or exceeds the permitted use, you will need to obtain permission directly from the copyright holder. To view a copy of this licence, visit <http://creativecommons.org/licenses/by/4.0/>.

## References

- Bear J (1972) Dynamics of fluids in porous media. American Elsevier Pub. Co.
- Berkowitz B, Zehe E (2020) Surface water and groundwater: unifying conceptualization and quantification of the two “water worlds.” *Hydrol Earth Syst Sci* 24(4):1831–1858. <https://doi.org/10.5194/hess-24-1831-2020>
- Bianchi M, Zheng CM, Wilson C, Tick GR, Liu GS, Gorelick SM (2011) Spatial connectivity in a highly heterogeneous aquifer: From cores to preferential flow paths. *Water Resour Res* 47:W05524. <https://doi.org/10.1029/2009wr008966>
- Blaschke AP, Derx J, Zessner M, Kirnbauer R, Kavka G, Strelec H, Farnleitner AH, Pang L (2016) Setback distances between small biological wastewater treatment systems and drinking water wells against virus contamination in alluvial aquifers. *Sci Total Environ* 573:278–289. <https://doi.org/10.1016/j.scitotenv.2016.08.075>
- Bloeschl G, Sivapalan M (1995) Scale issues in hydrological modeling - a review. *Hydrol Process* 9(3–4):251–290. <https://doi.org/10.1002/hyp.3360090305>
- Boggs JM, Adams EE (1992) Field-study of dispersion in a heterogeneous aquifer. 4. Investigation of adsorption and sampling bias. *Water Resour Res* 28(12):3325–3336. <https://doi.org/10.1029/92wr01759>
- Boggs JM, Young SC, Beard LM, Gelhar LW, Rehfeldt KR, Adams EE (1992) Field-study of dispersion in a heterogeneous aquifer. 1. Overview and site description. *Water Resour Res* 28(12):3281–3291. <https://doi.org/10.1029/92wr01756>
- Bradford SA, Harvey RW (2017) Future research needs involving pathogens in groundwater. *Hydrogeol J* 25(4):931–938. <https://doi.org/10.1007/s10040-016-1501-0>
- Bradford SA, Simunek J, Bettahar M, Van Genuchten MT, Yates SR (2003) Modeling colloid attachment, straining, and exclusion in saturated porous media. *Environ Sci Technol* 37(10):2242–2250. <https://doi.org/10.1021/es025899u>
- Bradford SA, Kim H, Headd B, Torkzaban S (2016) Evaluating the transport of *Bacillus subtilis* spores as a potential surrogate for *Cryptosporidium parvum* oocysts. *Environ Sci Technol* 50(3):1295–1303. <https://doi.org/10.1021/acs.est.5b05296>
- Cameron DR, Klute A (1977) Convective-dispersive solute transport with a combined equilibrium and kinetic adsorption model. *Water Resour Res* 13(1):183–188. <https://doi.org/10.1029/WR013i001p00183>
- Close ME, Pang L, Flintoft MJ, Sinton LW (2006) Distance and flow effects on microsphere transport in a large gravel column. *J Environ Qual* 35(4):1204–1212. <https://doi.org/10.2134/jeq2005.0286>
- de Graaf IEM, Sutanudjaja EH, van Beek LPH, Bierkens MFP (2015) A high-resolution global-scale groundwater model. *Hydrol Earth Syst Sci* 19(2):823–837. <https://doi.org/10.5194/hess-19-823-2015>
- DeBorde DC, Woessner WW, Lauerma B, Ball PN (1998) Virus occurrence and transport in a school septic system and unconfined aquifer. *Ground Water* 36(5):825–834. <https://doi.org/10.1111/j.1745-6584.1998.tb02201.x>
- Dong HL, Scheibe TD, Johnson WP, Monkman CM, Fuller ME (2006) Change of collision efficiency with distance in bacterial transport experiments. *Ground Water* 44(3):415–429. <https://doi.org/10.1111/j.1745-6584.2005.00133.x>
- Du X, Ostojca-Starzewski M (2006) On the size of representative volume element for Darcy law in random media. *Proc R Soc A-Math Phys Eng Sci* 462(2074):2949–2963. <https://doi.org/10.1098/rspa.2006.1704>
- Ederly Y, Guadagnini A, Scher H, Berkowitz B (2014) Origins of anomalous transport in heterogeneous media: structural and dynamic controls. *Water Resour Res* 50(2):1490–1505. <https://doi.org/10.1002/2013wr015111>
- Fiori A, Jankovic I (2012) On preferential flow, channeling and connectivity in heterogeneous porous formations. *Math Geosci* 44(2):133–145. <https://doi.org/10.1007/s11004-011-9365-2>
- Fiori A, Zarlenga A, Bellin A, Cvetkovic V, Dagan G (2019) Groundwater contaminant transport: prediction under uncertainty, with application to the MADE transport experiment. *Front Environ Sci* 7:79. <https://doi.org/10.3389/fenvs.2019.00079>
- Fogg GE, Zhang Y (2016) Debates-Stochastic subsurface hydrology from theory to practice: a geologic perspective. *Water Resour Res* 52(12):9235–9245. <https://doi.org/10.1002/2016wr019699>
- Freeze RA, Cherry JA (1979) *Groundwater*. Prentice-Hall

- Gelhar LW, Welty C, Rehfeldt KR (1992) A critical-review of data on field-scale dispersion in aquifers. *Water Resour Res* 28(7):1955–1974. <https://doi.org/10.1029/92wr00607>
- Gerke HH, Vangenuchten MT (1993) A dual-porosity model for simulating the preferential movement of water and solutes in structured porous-media. *Water Resour Res* 29(2):305–319. <https://doi.org/10.1029/92wr02339>
- Ghodrati M, Jury WA (1990) A field-study using dyes to characterize preferential flow of water. *Soil Sci Soc Am J* 54(6):1558–1563. <https://doi.org/10.2136/sssaj1990.03615995005400060008x>
- Gish TJ, Shirmohammadi A (1991) Preferential flow: proceedings of the national symposium: 16–17 December 1991, Chicago, Illinois. American Society of Agricultural Engineers
- Grindrod P, Edwards MS, Higgs JJW, Williams GM (1996) Analysis of colloid and tracer breakthrough curves. *J Contam Hydrol* 21(1–4):243–253. [https://doi.org/10.1016/0169-7722\(95\)00051-8](https://doi.org/10.1016/0169-7722(95)00051-8)
- Haggerty R, McKenna SA, Meigs LC (2000) On the late-time behavior of tracer test breakthrough curves. *Water Resour Res* 36(12):3467–3479. <https://doi.org/10.1029/2000wr900214>
- Harter T, Wagner S, Atwill ER (2000) Colloid transport and filtration of *Cryptosporidium parvum* in sandy soils and aquifer sediments. *Environ Sci Technol* 34(1):62–70. <https://doi.org/10.1021/Es990132w>
- Harvey RW, Kinner NE, Macdonald D, Metge DW, Bunn A (1993) Role of physical heterogeneity in the interpretation of small-scale laboratory and field observations of bacteria, microbial-sized microsphere, and bromide transport through aquifer sediments. *Water Resour Res* 29(8):2713–2721. <https://doi.org/10.1029/93wr00963>
- Hergarten S, Winkler G, Birk S (2014) Transferring the concept of minimum energy dissipation from river networks to subsurface flow patterns. *Hydrol Earth Syst Sci* 18(10):4277–4288. <https://doi.org/10.5194/hess-18-4277-2014>
- Hijnen WAM, Brouwer-Hanzens AJ, Charles KJ, Medema GJ (2005) Transport of MS2 phage, *Escherichia coli*, *Clostridium perfringens*, *Cryptosporidium parvum* and *Giardia intestinalis* in a gravel and a sandy soil. *Environ Sci Technol* 39(20):7860–7868. <https://doi.org/10.1021/es050427b>
- Hunt AG (2003) Some comments on the scale dependence of the hydraulic conductivity in the presence of nested heterogeneity. *Adv Water Resour* 26(1):71–77. [https://doi.org/10.1016/S0309-1708\(02\)00096-9](https://doi.org/10.1016/S0309-1708(02)00096-9)
- Johnson PR, Elimelech M (1995) Dynamics of colloid deposition in porous-media - blocking based on random sequential adsorption. *Langmuir* 11(3):801–812. <https://doi.org/10.1021/la00003a023>
- Kasnavia T, Vu D, Sabatini DA (1999) Fluorescent dye and media properties affecting sorption and tracer selection. *Ground Water* 37(3):376–381. <https://doi.org/10.1111/j.1745-6584.1999.tb0114.x>
- Knappett PS, Du J, Liu P, Horvath V, Mailloux BJ, Feighery J, van Geen A, Culligan PJ (2014) Importance of reversible attachment in predicting *E. coli* transport in saturated aquifers from column experiments. *Adv Water Resour* 63:120–130. <https://doi.org/10.1016/j.advwatres.2013.11.005>
- Kretzschmar R, Barmettler K, Grolimund D, Yan YD, Borkovec M, Sticher H (1997) Experimental determination of colloid deposition rates and collision efficiencies in natural porous media. *Water Resour Res* 33(5):1129–1137. <https://doi.org/10.1029/97wr00298>
- Lapidus L, Amundson NR (1952) Mathematics of adsorption in beds. 6. The effect of longitudinal diffusion in ion exchange and chromatographic columns. *J Phys Chem* 56(8):984–988. <https://doi.org/10.1021/j150500a014>
- Lin DT, Zhang XH, Hu LM, Bradford SA, Shen CY (2022) Prediction of colloid sticking efficiency at pore-scale and macroscale using a pore network model. *J Hydrol* 612:128253. <https://doi.org/10.1016/j.jhydrol.2022.128253>
- Logan BE, Jewett DG, Arnold RG, Bouwer EJ, Omelia CR (1995) Clarification of clean-bed filtration models. *J Environ Eng-Asce* 121(12):869–873. [https://doi.org/10.1061/\(Asce\)0733-9372\(1995\)121:12\(869\)](https://doi.org/10.1061/(Asce)0733-9372(1995)121:12(869))
- Lutterodt G, Basnet M, Foppen JW, Uhlenbrook S (2009) The effect of surface characteristics on the transport of multiple *Escherichia coli* isolates in large-scale columns of quartz sand. *Water Res* 43(3):595–604. <https://doi.org/10.1016/j.watres.2008.11.001>
- Lutterodt G, Foppen JWA, Maksoud A, Uhlenbrook S (2011) Transport of *Escherichia coli* in 25-m quartz sand columns. *J Contam Hydrol* 119(1–4):80–88. <https://doi.org/10.1016/j.jconhyd.2010.09.010>
- Mackay DM, Bianchimosquera G, Kopania AA, Kianjah H, Thorbjarnarson KW (1994) A forced-gradient experiment on solute transport in the Borden aquifer. 1. Experimental methods and moment analyses of results. *Water Resour Res* 30(2):369–383. <https://doi.org/10.1029/93wr02651>
- Martin MJ, Logan BE, Johnson WP, Jewett DG, Arnold RG (1996) Scaling bacterial filtration rates in different sized porous media. *J Environ Eng-Asce* 122(5):407–415. [https://doi.org/10.1061/\(Asce\)0733-9372\(1996\)122:5\(407\)](https://doi.org/10.1061/(Asce)0733-9372(1996)122:5(407))
- Matthess G, Pekdeger A, Schroeter J (1988) Persistence and transport of bacteria and viruses in groundwater — a conceptual evaluation. *J Contam Hydrol* 2(2):171–188. [https://doi.org/10.1016/0169-7722\(88\)90006-X](https://doi.org/10.1016/0169-7722(88)90006-X)
- Neuman SP (1990) Universal scaling of hydraulic conductivities and dispersivities in geologic media. *Water Resour Res* 26(8):1749–1758. <https://doi.org/10.1029/WR026i008p01749>
- Oudega TJ, Lindner G, Derx J, Farnleitner AH, Sommer R, Blaschke AP, Stevenson ME (2021) Upscaling transport of *Bacillus subtilis* endospores and coliphage phiX174 in heterogeneous porous media from the column to the field scale. *Environ Sci Technol* 55(16):11060–11069. <https://doi.org/10.1021/acs.est.1c01892>
- Oudega TJ, Lindner G, Sommer R, Farnleitner AH, Kerber G, Derx J, Stevenson ME, Blaschke AP (2022) Transport and removal of spores of *Bacillus subtilis* in an alluvial gravel aquifer at varying flow rates and implications for setback distances. *J Contam Hydrol* 251:104080. <https://doi.org/10.1016/j.jconhyd.2022.104080>
- Pang LP (2009) Microbial removal rates in subsurface media estimated from published studies of field experiments and large intact soil cores. *J Environ Qual* 38(4):1531–1559. <https://doi.org/10.2134/jeq2008.0379>
- Pang LP, Close M, Goltz M, Noonan M, Sinton L (2005) Filtration and transport of *Bacillus subtilis* spores and the F-RNA phage MS2 in a coarse alluvial gravel aquifer: Implications in the estimation of setback distances. *J Contam Hydrol* 77(3):165–194. <https://doi.org/10.1016/j.jconhyd.2004.12.006>
- Pang L, McLeod M, Aislabie J, Simunek J, Close M, Hector R (2008) Modeling transport of microbes in ten undisturbed soils under effluent irrigation. *Vadose Zone J* 7(1):97–111. <https://doi.org/10.2136/vzj2007.0108>
- Pieper AP, Ryan JN, Harvey RW, Amy GL, Illangasekare TH, Metge DW (1997) Transport and recovery of bacteriophage PRD1 in a sand and gravel aquifer: effect of sewage-derived organic matter. *Environ Sci Technol* 31(4):1163–1170. <https://doi.org/10.1021/Es960670y>
- Ptak T, Piepenbrink M, Martac E (2004) Tracer tests for the investigation of heterogeneous porous media and stochastic modelling of flow and transport - a review of some recent developments. *J Hydrol* 294(1–3):122–163. <https://doi.org/10.1016/j.jhydrol.2004.01.020>

- Redman JA, Grant SB, Olson TM, Estes MK (2001) Pathogen filtration, heterogeneity, and the potable reuse of wastewater. *Environ Sci Technol* 35(9):1798–1805. <https://doi.org/10.1021/es0010960>
- Riva M, Guadagnini A, Fernandez-Garcia D, Sanchez-Vila X, Ptak T (2008) Relative importance of geostatistical and transport models in describing heavily tailed breakthrough curves at the Lauswiesen site. *J Contam Hydrol* 101(1–4):1–13. <https://doi.org/10.1016/j.jconhyd.2008.07.004>
- Schiavo M, Riva M, Guadagnini L, Zehe E, Guadagnini A (2022) Probabilistic identification of preferential groundwater networks. *J Hydrol* 610:127906. <https://doi.org/10.1016/j.jhydrol.2022.127906>
- Schijven JF, Hassanizadeh SM (2000) Removal of viruses by soil passage: overview of modeling, processes, and parameters. *Crit Rev Environ Sci Technol* 30(1):49–127. <https://doi.org/10.1080/10643380091184174>
- Schijven JF, Simunek J (2002) Kinetic modeling of virus transport at the field scale. *J Contam Hydrol* 55(1–2):113–135. [https://doi.org/10.1016/S0169-7722\(01\)00188-7](https://doi.org/10.1016/S0169-7722(01)00188-7)
- Schijven JF, Hoogenboezem W, Hassanizadeh SM, Peters JH (1999) Modeling removal of bacteriophages MS2 and PRD1 by dune recharge at Castricum, Netherlands. *Water Resour Res* 35(4):1101–1111. <https://doi.org/10.1029/1998wr900108>
- Schijven JF, Medema G, Vogelaar AJ, Hassanizadeh SM (2000) Removal of microorganisms by deep well injection. *J Contam Hydrol* 44(3–4):301–327. [https://doi.org/10.1016/S0169-7722\(00\)00098-X](https://doi.org/10.1016/S0169-7722(00)00098-X)
- Schijven JF, Hassanizadeh SM, de Bruin HAM (2002a) Column experiments to study nonlinear removal of bacteriophages by passage through saturated dune sand. *J Contam Hydrol* 58(3–4):243–259. [https://doi.org/10.1016/S0169-7722\(02\)00040-2](https://doi.org/10.1016/S0169-7722(02)00040-2)
- Schijven JF, Hassanizadeh SM, de Bruin RHAM (2002b) Two-site kinetic modeling of bacteriophages transport through columns of saturated dune sand. *J Contam Hydrol* 57(3–4):259–279. [https://doi.org/10.1016/S0169-7722\(01\)00215-7](https://doi.org/10.1016/S0169-7722(01)00215-7)
- Schulze-Makuch D, Carlson DA, Cherkauer DS, Malik P (1999) Scale dependency of hydraulic conductivity in heterogeneous media. *Ground Water* 37(6):904–919. <https://doi.org/10.1111/j.1745-6584.1999.tb01190.x>
- Schumer R, Benson DA, Meerschaert MM, Baeumer B (2003) Fractal mobile/immobile solute transport. *Water Resour Res* 39(10):1296. <https://doi.org/10.1029/2003wr002141>
- Simoni SF, Harms H, Bosma TNP, Zehnder AJB (1998) Population heterogeneity affects transport of bacteria through sand columns at low flow rates. *Environ Sci Technol* 32(14):2100–2105. <https://doi.org/10.1021/es970936g>
- Simunek J, Jacques D, Langergraber G, Bradford SA, Sejna M, van Genuchten MT (2013) Numerical modeling of contaminant transport using HYDRUS and its specialized modules. *J Indian Inst Sci* 93(2):265–284. <Go to ISI>://WOS:000322245700010
- Smith L, Freeze RA (1979) Stochastic-analysis of steady-state groundwater-flow in a bounded domain. 2. Two-dimensional simulations. *Water Resour Res* 15(6):1543–1559. <https://doi.org/10.1029/WR015i006p01543>
- Stevenson ME, Blaschke AP, Schauer S, Zessner M, Sommer R, Farnleitner AH, Kirschner AKT (2014) Enumerating microorganism surrogates for groundwater transport studies using solid-phase cytometry. *Water Air Soil Pollut* 225(2):1827. <https://doi.org/10.1007/S11270-013-1827-3>
- Stevenson ME, Sommer R, Lindner G, Farnleitner AH, Toze S, Kirschner AK, Blaschke AP, Sidhu JP (2015) Attachment and detachment behavior of human adenovirus and surrogates in fine granular limestone aquifer material. *J Environ Qual* 44(5):1392–1401. <https://doi.org/10.2134/jeq2015.01.0052>
- Stevenson ME, Kumpan M, Feichtinger F, Scheidl A, Eder A, Durner W, Blaschke AP, Strauss P (2021a) Innovative method for installing soil moisture probes in a large-scale undisturbed gravel lysimeter. *Vadose Zone J* 20(1):e20106. <https://doi.org/10.1002/vzj2.20106>
- Stevenson ME, Kumpan M, Feichtinger F, Scheidl A, Eder A, Durner W, Blaschke AP, Strauss P (2021b) Innovative installation of soil moisture sensors in an indoor gravel lysimeter. <https://doi.org/10.5061/dryad.mw6m905vz>
- Tarboton DG, Bras RL, Rodriguez-Iturbe I (1989) Scaling and elevation in river networks. *Water Resour Res* 25(9):2037–2051. <https://doi.org/10.1029/WR025i009p02037>
- Theis, C. V. (1967). Aquifers and models. In: Symposium on groundwater hydrology, San Francisco, USA. American Water Resources Association Proceedings Series, vol. 4. pp 138–148
- Tirafferri A, Tosco T, Sethi R (2011) Transport and retention of microparticles in packed sand columns at low and intermediate ionic strengths: experiments and mathematical modeling. *Environ Earth Sci* 63(4):847–859. <https://doi.org/10.1007/s12665-010-0755-4>
- Tufenkji N (2006) Application of a dual deposition mode model to evaluate transport of D21 in porous media. *Water Resour Res* 42(12):W12s11. <https://doi.org/10.1029/2005wr004851>
- Tufenkji N, Elimelech M (2004) Correlation equation for predicting single-collector efficiency in physicochemical filtration in saturated porous media. *Environ Sci Technol* 38(2):529–536. <https://doi.org/10.1021/Es034049r>
- Wheatcraft SW, Tyler SW (1988) An explanation of scale-dependent dispersivity in heterogeneous aquifers using concepts of fractal geometry. *Water Resour Res* 24(4):566–578. <https://doi.org/10.1029/WR024i004p00566>
- Wymore AS, Larsen W, Kincaid DW, Underwood KL, Fazekas HM, McDowell WH, Murray DS, Shogren AJ, Speir SL, Webster AJ (2023) Revisiting the origins of the power-law analysis for the assessment of concentration–discharge relationships. *Water Resour Res* 59(8):e2023WR034910. <https://doi.org/10.1029/2023WR034910>
- Yao KM, Habibian MT, O’melia CR (1971) Water and waste water filtration: concepts and applications. *Environ Sci Technol* 5(11):1105–1112. <https://doi.org/10.1021/es60058a005>
- Zehe E, Loritz R, Edery Y, Berkowitz B (2021) Preferential pathways for fluid and solutes in heterogeneous groundwater systems: self-organization, entropy, work. *Hydrol Earth Syst Sci* 25(10):5337–5353. <https://doi.org/10.5194/hess-25-5337-2021>

**Publisher's Note** Springer Nature remains neutral with regard to jurisdictional claims in published maps and institutional affiliations.